Molecular Crystals and Liquid Crystals

Publication details, including instructions for authors and subscription information:
http://www.tandfonline.com/loi/gmcl20

A Novel Approach to the Normal Force in Shear of Nematic Liquid Crystals in the Cone-and-Plate Rheometer

Assis F. Martins [a] & Alain R. Véron [a]

[a] Dpt. Ciência dos Materiais and I3N/CENIMAT, Faculdade de Ciências e Tecnologia, Universidade Nova de Lisboa, Caparica, Portugal

Version of record first published: 30 Jan 2009

To cite this article: Assis F. Martins & Alain R. Véron (2008): A Novel Approach to the Normal Force in Shear of Nematic Liquid Crystals in the Cone-and-Plate Rheometer, Molecular Crystals and Liquid Crystals, 495:1, 312/[664]-333/[685]

To link to this article: http://dx.doi.org/10.1080/15421400802430422

Mol. Cryst. Liq. Cryst., Vol. 495, pp. 312/[664]–333/[685], 2008

ISSN: 1542-1406 print/1563-5287 online
DOI: 10.1080/15421400802430422

A Novel Approach to the Normal Force in Shear of Nematic Liquid Crystals in the Cone-and-Plate Rheometer

Assis F. Martins and Alain R. Véron
Dpt. Ciência dos Materiais and I3N/CENIMAT, Faculdade de Ciências e Tecnologia, Universidade Nova de Lisboa, Caparica, Portugal

We reexamine the interpretation of the normal force measured with a cone-and-plate rheometer for nematic liquid crystals. We point out the fact that the quite widespread belief that the normal force is directly related to the well-known rheological function $\mathcal{N}_1$ (i.e., the first normal stress difference) fails for these complex fluids. After a brief presentation of the theoretical bases leading to the general expression of the normal force, this new approach is applied to nematic liquid crystals within the framework of Leslie-Ericksen theory. In order to avoid heavy numerical computations the full Leslie-Ericksen equations describing the three-dimensional flow within the cone-and-plate cell are reduced, thanks to reasonable approximations, to an effective one-dimensional problem (i.e., a system of partial differential equations with spatial derivatives with respect to one single coordinate). Results for low molecular weight liquid crystals are presented and discussed. The main feature evidenced in this work is the notable difference between the normal force calculated in this way and the $\mathcal{N}_1$ function, in particular the normal force function becomes negative for high shear rate while $\mathcal{N}_1$ stays positive.

Keywords: cone-and-plate; Leslie-Ericksen; nematic; normal force; shear

I. INTRODUCTION

Rheological measurements constitute a powerful tool to test constitutive equations; it is in particular the case for the measurement of the normal force with a cone-and-plate rheometer. Nevertheless

This work was partly supported by "Fundação para a Ciência e a Tecnologia" through a research grant to A. Véron.

Address correspondence to Assis F. Martins, Dpt. Ciência dos Materiais, Faculdade de Ciências e Tecnologia, Universidade Nova de Lisboa, 2829-516 Caparica, Portugal. E-mail: asfm@fct.unl.pt

the exploitation of the experimental data obviously requires a clear theoretical model for the normal force. It is the purpose of this paper to analyse theoretically this topic for nematic liquid crystals within the frame-work of Leslie-Ericksen theory that describes the hydrodynamics of these fluids. It will be shown that the complex character of liquid crystals entrains that the normal force is not simply related to the first normal stress difference, i.e., the $\mathcal{N}_1$ function, as usually admitted for isotropic liquids. In this work we focus our attention on an additional contribution that exists in general and we show that it cannot be neglected for liquid crystals.

In the following, we first give an expression for the normal force when (i) inertia is neglected, (ii) the flow possesses the cylindrical symmetry of the cone-and-plate set-up and (iii) the extra stress tensor is independent of the radius. Subsequently this result is applied to nematics, which requires solving the Leslie-Ericksen equations of motion for the quite complex cone-and-plate geometry. In order to avoid large time consuming computations, a simple one-dimensional model is derived from the general theory. To this end some reasonable hypotheses concerning the radial dependence of the flow will be made. The resulting model is applied to MBBA.

II. NORMAL FORCE AND PRESSURE IN THE CONE-AND-PLATE CELL

The total stress tensor σ is separated in two parts as follows

$$\sigma_{\alpha\beta} = -p\delta_{\alpha\beta} + \tau_{\alpha\beta} \tag{1}$$

where τ denotes the extra stress tensor and p the pressure. The equations of motion are written in a convenient system of spherical coordinates (r, θ, ϕ)[1] associated to the cone-and-plate cell; its origin coincides with the contact point between the cone and the plate, the symmetry axis of the cell is chosen as the polar axis and the origin of the azimuthal angle ϕ is let arbitrary. The fluid occupies the volume defined by $0 \leq r \leq R$ and $\pi/2 - \beta_c \leq \theta \leq \pi/2$ where R is the radius of the cell and β_c the angle between the cone and the plate (see Fig. 1). When (i) inertia is neglected, (ii) the flow possess the axial symmetry of the cone-and-plate cell ($\partial\sigma/\partial r = 0$) and (iii) the extra stress tensor τ is independent of the radius ($\partial\tau/\partial r = 0$) the equations of motion in spherical coordinates reduce to [1]

[1] r: radius; θ: polar angle; ϕ: azimuthal angle.

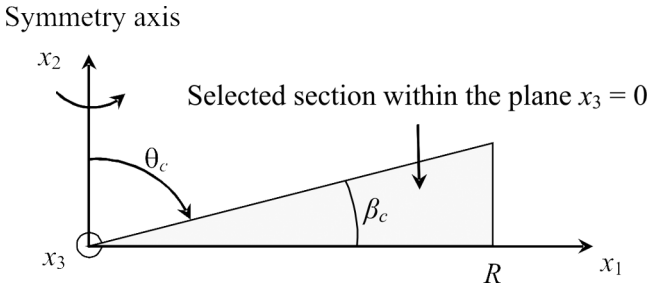

FIGURE 1 System of Cartesian axes used to describe the flow inside a cone-and-plate cell; R: radius of the cell, β_c: angle between the cone and the plate. When the flow is axy-symmetric with respect to the x_2 axis the whole flow is fully defined by the flow characteristics within the gray triangular section.

$$\begin{cases} -r\frac{\partial p}{\partial r} + \frac{\partial \tau_{\theta r}}{\partial \theta} + 2\tau_{rr} - \tau_{\theta\theta} - \tau_{\phi\phi} + \cot\theta\ \tau_{\theta r} = 0 & \text{(a)} \\ -\frac{\partial p}{\partial \theta} + \frac{\partial \tau_{\theta\theta}}{\partial \theta} + 2\tau_{r\theta} + \tau_{\theta r} + \cot\theta(\tau_{\theta\theta} - \tau_{\phi\phi}) = 0 & \text{(b)} \\ \frac{\partial \tau_{\theta\phi}}{\partial \theta} + 2\tau_{r\phi} + \tau_{\phi r} + \cot\theta(\tau_{\phi\theta} + \tau_{\theta\phi}) = 0 & \text{(c)} \end{cases} \tag{2}$$

The total normal force $F_c(t)$ on the cone reads

$$F_c(t) = 2\pi \int_0^R (p(t,r,\theta_c) - \tau_{\theta\theta}(t,\theta_c))r dr \tag{3}$$

Integration by parts of the pressure term in Eq. (3) yields

$$F_c(t) = \pi R^2 p(t,R,\theta_c) - 2\pi \int_0^R \left(\frac{r}{2}\frac{\partial p(t,r,\theta_c)}{\partial r} + \tau_{\theta\theta}(t,\theta_c)\right) r dr \tag{4}$$

By inserting the expression of $\partial p/\partial r$ derived from Eq. (2a) into Eq. (4) and using $\partial \tau/\partial r = 0$ we get

$$F_c(t) = \pi R^2 \left(p(t,R,\theta_c) - \tau_{rr} + \frac{1}{2}\left(\tau_{\phi\phi} - \tau_{\theta\theta} - \frac{\partial \tau_{\theta r}}{\partial \theta} - \cot\theta\ \tau_{\theta r}\right)\right) \tag{5}$$

At the edge of the cell the fluid is in equilibrium with the atmosphere at pressure p_0, which entrains

$$p(t,R,\theta_c) - \tau_{rr}(t,\theta_c) = p_0 \tag{6}$$

Finally the normal force exerted by the fluid on the cone reads

$$F_c(t) = \pi R^2 \left(p_0 + \frac{1}{2}\mathcal{N}_{1eff}(t,\theta_c)\right) \tag{7}$$

with

$$\mathcal{N}_{1eff} = \mathcal{N}_1 + \Delta\mathcal{N}_1 \tag{8}$$

where $\mathcal{N}_1$ is the well-known first normal stress difference defined by

$$\mathcal{N}_1 = \sigma_{\phi\phi} - \sigma_{\theta\theta} = \tau_{\phi\phi} - \tau_{\theta\theta} \tag{9}$$

and

$$\Delta\mathcal{N}_1 = -\frac{\partial \tau_{\theta r}}{\partial \theta} - \cot\theta\ \tau_{\theta r} \tag{10}$$

By differentiating Eqs. (2a) and (2b) with respect to r and using $\partial\tau/\partial r = 0$ we get

$$\begin{cases} \frac{\partial}{\partial r}\left(r\frac{\partial p}{\partial r}\right) = 0 & \text{(a)} \\ \frac{\partial^2 p}{\partial r \partial \theta} = 0 & \text{(b)} \end{cases} \tag{11}$$

Integration of Eq. (11a) yields $r\partial p/\partial r = k(\theta, t)$ with $k(\theta, t)$ an arbitrary function of θ and t; by inserting this result in Eq. (11b) we get $\partial k/\partial\theta = 0$ and consequently

$$r\frac{\partial p}{\partial r} = k(t) \tag{12}$$

where $k(t)$ is independent of space. Finally by combining Eq. (12) with Eq. (2a) we get the following new expression for $\Delta\mathcal{N}_1$ initially defined by Eq. (10)

$$\Delta\mathcal{N}_1 = 2\tau_{rr} - \tau_{\theta\theta} - \tau_{\phi\phi} - k \tag{13}$$

III. A SIMPLE MODEL FOR NEMATIC FLOW BETWEEN CONE AND PLATE

In order to evaluate the normal force, or equivalently $\mathcal{N}_{1eff}$ according to Eq. (7), it is necessary to solve the equations of motion with a constitutive equation defining the extra stress tensor τ. For low molecular weight nematics the well-known Leslie-Ericksen theory [2,3] applies. However, in order to minimize time consuming computations a simple model that describes the flow of nematics between cone and plate is derived from the general theory. On the other hand, for the sake of simplicity Cartesian coordinates are used in the sequel.

III.1. Leslie-Ericksen Theory

When convective contributions are neglected, i.e., when $d/dt \approx \partial/\partial t$ the extra stress tensor τ reads

$$\tau_{ij} = L_{ijpq} V_{p,q} + S_{ij} \quad (i,j,p,q = 1,2,3) \tag{14}$$

with

$$L_{ijpq} = \frac{1}{2} \left\{ \begin{array}{c} 2\alpha_1 n_i n_j n_p n_q + \alpha_4(\delta_{ip}\delta_{jq} + \delta_{iq}\delta_{jp}) \\ +(\alpha_5 + \alpha_2) n_i n_p \delta_{jq} + (\alpha_5 - \alpha_2) n_i n_q \delta_{jp} \\ +(\alpha_6 + \alpha_3) n_j n_p \delta_{iq} + (\alpha_6 - \alpha_3) n_j n_q \delta_{ip} \end{array} \right\} \tag{15}$$

and

$$S_{ij} = \alpha_2 n_i \frac{\partial n_j}{\partial t} + \alpha_3 n_j \frac{\partial n_i}{\partial t} + \tau^e_{ij} \tag{16}$$

where τ^e_{ij} denotes the Ericksen stress tensor defined by

$$\tau^e_{ij} = -K_2 n_{k,i} n_{k,j} - (K_1 - K_2) n_{l,l} n_{i,j} - (K_3 - K_2) n_i n_l n_{k,l} n_{k,j} \tag{17}$$

In Eqs. (14) to (17) V_p ($p = 1, 2, 3$) denotes the pth component of the velocity, α_i ($i = 1, \ldots, 6$) the Leslie viscosities[2], n_i ($i = 1, 2, 3$) the ith component of the director and finally K_1, K_2 and K_3 denote the Frank elastic constants.

In the Leslie-Ericksen theory the director $\vec{n}$ obeys to the following time evolution equation

$$\gamma_1 \frac{\partial n_i}{\partial t} = -\alpha_2 n_q V_{i,q} - \alpha_3 n_p V_{p,i} + h_i + \lambda n_i \quad (i,p,q = 1,2,3) \tag{18}$$

where $\gamma_1 = \alpha_3 - \alpha_2$, λ is a Lagrangian multiplier associated with the condition $\vec{n} \cdot \vec{n} = 1$ and $\vec{h}$ is the so-called molecular field associated with Frank elasticity and defined by

$$\begin{aligned} h_i = {} & K_2 n_{i,jj} + (K_1 - K_2) n_{j,ji} + (K_3 - K_2)(n_j n_{i,j} n_{k,k} + n_j n_k n_{i,jk} \\ & + n_{i,j} n_k n_{j,k} - n_j n_{k,j} n_{k,i}) \end{aligned} \tag{19}$$

III.2. Basic Assumptions Leading to a One-Dimensional Model

Because of axial symmetry it is sufficient to determine the flow characteristics within one single planar section of the cone-and-plate cell containing the symmetry axis as shown in Figure 1. Once such an arbitrary section has been selected we define right-handed Cartesian axes as follows: the x_1 axis is chosen within the selected section and normal to the symmetry axis, the x_2 axis coincides with the symmetry

[2]The Leslie viscosities satisfy the Parodi relation $\alpha_2 + \alpha_3 = \alpha_6 - \alpha_5$.

axis and the x_3 axis is taken normal to the selected section. Moreover the contact point between the plate and the cone defines the origin of the coordinates system (see Fig. 1). Because of axial symmetry the derivatives $\partial T_{ij\cdots}/\partial x_3|_{x_3=0}$ of any tensor T are well-defined functions of the tensor T itself; the list of these derivatives useful for this work is given in Appendix I.

Concerning the velocity profile we neglect any flow normal to the plates, i.e., we assume $V_2 = 0$. On the contrary, the possibility of 'radial' flow, i.e., $V_1 \neq 0$, is considered in order to be consistent with occurrence of well-established backflow along the vorticity axis for infinite parallel plates [4]. However, the finite size of the set-up imposes $V_1 = 0$ at the fluid/air interface. Accordingly at least one roll must develop within the cell, which entrains that V_2 cannot vanish everywhere. For that reason we assume that our model is valid sufficiently far from the centre and the fluid/air interface (i.e., for $x_1 \in [\xi, R - \xi]$ with $0 < \xi << R$).

Since the basic equations of Leslie-Ericksen theory are given in Cartesian coordinates, we are lead to convert the equations of Section II from spherical coordinates towards Cartesian coordinates. To this end we give in Appendix II the useful relations allowing this conversion when the variables are evaluated within the plane $x_3 = 0$. Using moreover the approximation $\sin\theta \approx 1$ and $\cos\theta \approx 0$[3] Eqs. (II-1) to (II-3) yield

$$\begin{cases} \frac{\partial \tau_{\theta r}}{\partial \theta} + \cot\theta\ \tau_{\theta r} + 2\tau_{rr} - \tau_{\theta\theta} - \tau_{\phi\phi} \approx x_1 \frac{\partial \tau_{21}}{\partial x_2} + \tau_{11} - \tau_{33} \\ \frac{\partial \tau_{\theta\phi}}{\partial \theta} + 2\tau_{r\phi} + \tau_{\phi r} \approx -x_1 \frac{\partial \tau_{23}}{\partial x_2} - \tau_{13} - \tau_{31} \end{cases} \tag{20}$$

When Eqs. (12) and (20) are used the two equations of motion, Eqs. (2a) and (2c), may be approximated by

$$\begin{cases} x_1 \frac{\partial \tau_{21}}{\partial x_2} + \tau_{11} - \tau_{33} - k = 0 & \text{(a)} \\ x_1 \frac{\partial \tau_{23}}{\partial x_2} + \tau_{13} + \tau_{31} = 0 & \text{(b)} \end{cases} \tag{21}$$

It is worth pointing out that Eq. (21) is valid only within the plane $x_3 = 0$ because the expressions in Appendix II used to derive Eq. (20) are valid only within this particular plane. Actually this restriction is only apparent since axial symmetry entrains that the solution of Eq. (21) may be extended to the whole sample by rotation around the x_2 axis. On the other hand since we assume $V_2 = 0$ we only need two equations to determine V_1 and V_3; in order to avoid the determination of the pressure we have interest in using Eq. (2a) instead of

[3]In practice, the angle between the cone and the plate is very small, in the order of 10^{-3} rad.

Eq. (2b) because in the former equation the pressure term reduces to one constant in space instead of an arbitrary function. Finally the presence of the coordinate x_1 in Eq. (21) may appear in contradiction with the assumption $\partial\tau/\partial r = 0$; actually it is not the case; indeed, using the operator relation $r\partial../\partial r = x_1\partial../\partial x_1 + x_2\partial../\partial x_2$ on can readily show that $\partial\tau_{ij}/\partial r = 0$ implies $x_1\partial\tau_{ij}/\partial x_2$ independent of the radius.

Because of axial symmetry, the spatial derivatives with respect to x_3 appearing in the expressions of τ_{ij} and $\partial\tau_{ij}/\partial x_2$ (see Eqs. (14) to (17)) may be eliminated by using the relations given in Appendix I. It follows that the resolution of Eq. (21) within the planar section depicted by Figure 1 becomes a pure two-dimensional problem involving uniquely the coordinates x_1 and x_2. However, in order to avoid time consuming numerical calculations we intend to restrict this two-dimensional problem into a one-dimensional problem. More precisely, we are seeking for differential equations involving only the spatial derivatives with respect to x_2. To reach this objective we need to 'eliminate' the spatial derivatives with respect to x_1 appearing in the expressions of τ_{ij} and $\partial\tau_{ij}/\partial x_2$. This task requires particular attention. It should be recalled that the results of section II have been obtained by assuming τ independent of the radius. Noting that within the cone-and-plate cell both coordinates r and x_1 almost coincide we may conclude that τ is approximately independent of x_1. To fulfill this latter requirement Eqs. (14) to (19) suggest to impose n_i and $V_{i,j}$ $(i, j = 1, 2, 3)$ (at least approximately) independent of x_1. Concerning the director, we simply cancel the terms $n_{i,1}$ and $n_{i,j1}$ ($i = 1, 2, 3$ and $j = 1, 2$[4]) in Eqs. (17) and (19). Concerning the velocity, it turns out that the combination of axial symmetry, incompressibility and $V_2 = 0$ entrains that $V_{1,2}, V_{1,22}, V_{3,2}, V_{3,22}, V_{3,1}, V_{3,11}, V_{3,21}$ determine the remaining first and second spatial derivatives of V_1 and V_3. Since $V_{1,2}$, $V_{1,22}, V_{3,2}, V_{3,22}$ are variables of the one-dimensional model we are seeking for we have to impose $V_{3,1}, V_{3,11}, V_{3,21}$. Because of the non-slippage boundary condition for the velocity we expect V_3 to be approximately proportional to x_1 within the whole sample. Accordingly, we are lead to impose

$$\begin{cases} V_{3,1} \approx V_3/x_1 & \text{(a)} \\ V_{3,11} \approx 0 & \text{(b)} \\ V_{3,21} \approx 0 & \text{(c)} \end{cases} \tag{22}$$

where Eq. (22a) results from $V_3 \propto x_1$ while Eqs. (22b) and (22c) result from $V_{3,1}$ and $V_{3,2}$ approximately independent of x_1. Finally we give in

[4]The case $j = 3$ is given by Eq. (I-3) because of axial symmetry.

Appendix III the expressions of all the velocity gradients other than $V_{1,2}$, $V_{1,22}$, $V_{3,2}$, $V_{3,22}$.

III.3 Velocity Equations

When the spatial derivatives of the velocity given by Eqs. (III-3) to (III-5) are inserted into Eq. (14) we get

$$\tau_{ij} = L^*_{ij1}V_1 + L^*_{ij12}V_{1,2} + L^*_{ij3}V_3 + L^*_{ij32}V_{3,2} + S_{ij} \tag{23}$$

and

$$\frac{\partial \tau_{ij}}{\partial x_2} = L^\#_{ij1}V_1 + L^\#_{ij12}V_{1,2} + L^\#_{ij122}V_{1,22} + L^\#_{ij3}V_3 + L^\#_{ij32}V_{3,2} + L^\#_{ij322}V_{3,22} + \frac{\partial S_{ij}}{\partial x_2} \tag{24}$$

with

$$\begin{cases} L^*_{ij1} = \frac{1}{x_1}(L_{ij33} - L_{ij11}) \\ L^*_{ij12} = L_{ij12} \end{cases} \qquad \begin{cases} L^*_{ij3} = \frac{1}{x_1}(L_{ij31} - L_{ij13}) \\ L^*_{ij32} = L_{ij32} \end{cases} \tag{25}$$

and

$$\begin{cases} L^\#_{ij1} = \frac{1}{x_1}(L_{ij33,2} - L_{ij11,2}) \\ L^\#_{ij12} = L_{ij12,2} + \frac{1}{x_1}(L_{ij33} - L_{ij11}) \\ L^\#_{ij122} = L_{ij12} \end{cases} \qquad \begin{cases} L^\#_{ij3} = \frac{1}{x_1}(L_{ij31,2} - L_{ij13,2}) \\ L^\#_{ij32} = L_{ij32,2} - \frac{L_{ij13}}{x_1} \\ L^\#_{ij322} = L_{ij32} \end{cases} \tag{26}$$

Equation (21) may be rewritten as

$$\begin{cases} C_{11}V_{1,2} + C_{13}V_{3,2} + D_{11}V_{1,22} + D_{13}V_{3,22} + J_{11}V_1 + J_{13}V_3 + S_1 = 0 & \text{(a)} \\ C_{31}V_{1,2} + C_{33}V_{3,2} + D_{31}V_{1,22} + D_{33}V_{3,22} + J_{31}V_1 + J_{33}V_3 + S_3 = 0 & \text{(b)} \end{cases} \tag{27}$$

with

$$\begin{cases} J_{11} = L^\#_{211} + \frac{1}{x_1}(L^*_{111} - L^*_{331}) \\ J_{13} = L^\#_{213} + \frac{1}{x_1}(L^*_{113} - L^*_{333}) \\ S_1 = \frac{\partial S_{21}}{\partial x_2} + \frac{S_{11} - S_{33} - k}{x_1} \end{cases} \qquad \begin{cases} C_{11} = L^\#_{2112} + \frac{1}{x_1}(L^*_{1112} - L^*_{3312}) \\ C_{13} = L^\#_{2132} + \frac{1}{x_1}(L^*_{1132} - L^*_{3332}) \\ D_{11} = L^\#_{21122} \\ D_{13} = L^\#_{21322} \end{cases} \tag{28}$$

and

$$\begin{cases} J_{31} = L^{\#}_{231} + \frac{1}{x_1}(L^{*}_{131} + L^{*}_{311}) \\ J_{33} = L^{\#}_{233} + \frac{1}{x_1}(L^{*}_{133} + L^{*}_{313}) \\ S_3 = \frac{\partial S_{23}}{\partial x_2} + \frac{S_{13}+S_{31}}{x_1} \end{cases} \qquad \begin{cases} C_{31} = L^{\#}_{2312} + \frac{1}{x_1}(L^{*}_{1312} + L^{*}_{3112}) \\ C_{33} = L^{\#}_{2332} + \frac{1}{x_1}(L^{*}_{1332} + L^{*}_{3132}) \\ D_{31} = L^{\#}_{23122} \\ D_{33} = L^{\#}_{23322} \end{cases} \tag{29}$$

The last stage consists in determining the space constant $k(t)$ included in the coefficient S_1 of Eq. (28). We note that natural boundary conditions at the edge of the cell (i.e. $V_1 = 0$) combined with the incompressibility condition impose null net flux of the fluid along the x_1 direction. Clearly, for a given director configuration at a given time t (i.e. for given coefficients C_{ab}, D_{ab}, J_{ab} and S_a (a, $b = 1, 3$) in Eq. (27)) the net flux of fluid along x_1 is a function of k that we note $\Phi(t,k)$ and is defined by

$$\Phi(t,k) = \int_0^d V_1(t,x_2;k)\,dx_2 \tag{30}$$

where $V_1(t,x_2;k)$ denotes the solution of Eq. (27) for a fixed value of k. It follows that at any time t the constant k must be adjusted in order to satisfy the condition $\Phi(t, k) = 0$, which defines $k(t)$.

IV. RESULTS AND DISCUSSION

The continuum equations for the director and the velocity, namely Eqs. (18) and (27) respectively, are discretised and solved numerically. For both equations a centered finite difference scheme is used for spatial derivatives. The discretisation of Eq. (27) leads to a system of linear equations with respect to the velocity characterized by a tridiagonal matrix, such a linear system is efficiently solved by employing the Thomas algorithm [5]. On the other hand the discretisation of spatial derivatives in the director equation yields a set of differential equations with respect to time, this system is solved using the Runge-Kutta method. At any time Eq. (27) is solved for a fixed constant k and the net flux $\Phi(k)$ is calculated by integrating the component $V_1(x_2;k)$ over the sample depth using the trapezoidal method. Subsequently the equation $\Phi(k) = 0$ is solved by using the Newton's method. Finally $\Delta\mathcal{N}_1$ is calculated with Eq. (13) converted to Cartesian coordinates thanks to Eq. (II-1). Non-rigid boundary conditions have been used for the director. It means that the director on the plates

can go away from a particular direction called the easy axis with a finite energetic cost related to the anchoring strength A_s. This approach, detailed in Appendix IV, leads to the director boundary conditions expressed by Eq. (IV-5).

The orientation of the surface easy axis $\vec{e}$ is specified by the angles β_n and ψ_n as follows

$$\begin{cases} e_1 = \cos\psi_n \sin\beta_n \\ e_2 = \sin\psi_n \sin\beta_n \\ e_3 = \cos\beta_n \end{cases} \tag{31}$$

On the other hand, Eqs. (18) and (27) are solved for a given coordinate x_1 (see Fig. 1) and a given depth d such that $\tan\beta_c = d/x_1$ where β_c is the angle between the cone and the plate. The values of β_n, ψ_n, A_s, d and x_1 used in this work are given in Table 1. They correspond to quasi homeotropic anchoring[5] and to $\beta_c = 7.50 \times 10^{-3}$ rd (0.43°). On the other hand the anchoring strength A_s is consistent with experimental data [6]. The material parameters (i.e. $\alpha_1, \ldots, \alpha_6$ and K_1, K_2, K_3) used in this work are given in Table 2. The Leslie viscosities correspond to MBBA at 40°C [7] while the elastic constants are those of 5CB [8].

Figure 2 shows the steady director profile for three values of the shear rate. The director tends to align with the main velocity in the bulk, especially for high shear rate ($n_3 \approx 1$ in Fig. 2c), while it tends to keep the easy axis orientation on the bounding plates because of anchoring ($n_2 \approx 1$ in Fig. 2b). Consequently, strong director gradients occur within two boundary layers whose depth decreases with increasing shear rate (see Figs. 2b and 2c). In the bulk, the angle θ between the director and the main velocity (i.e. the x_3 axis) equals the Leslie angle θ_L defined by $\tan\theta_L = \sqrt{\alpha_3/\alpha_2}$. The most unusual feature is the non-vanishing component n_1 especially close to the cone as shown by Figure 2a, which means that the director stabilizes out of the shear plane. It is possible to show that it is an effect of the flow curvature that generates the velocity gradient $V_{1,3}$ in the director equation (Eq. (18)). Indeed, by canceling this contribution in Eq. (18), we observe that the director stays much closer to the shear plane. Another interesting feature is evidenced, namely, the smaller the viscosity α_3 in absolute value the stronger the tendency of the director to escape from the shear plane. It is even possible to get n_1 close to 1 in some part of the sample for very small values of $|\alpha_3|$.

Figures 3 and 4 show the first and second derivatives of the two non-null velocity components V_1 and V_3 with respect to x_2 in the

[5]This choice is complete with an initial homogeneous condition exhibiting axial symmetry.

TABLE 1 Model Parameters Used in this Work

β_n(rd)	ψ_n(rd)	$d(\mu m)$	x_1(mm)	A_s(J m^{-2})
1.57	1.57	300	40	3.5×10^{-6}

TABLE 2 Material Parameters Used in this Work. The Viscosities $\alpha_i (i = 1, \ldots, 6)$ are in Pa s and the Elastic Constants $K_i (i = 1, 2, 3)$ are in Jm^{-1}

α_1	α_2	α_3	α_4	α_5	α_6
-5.40×10^{-3}	-3.87×10^{-2}	-2.23×10^{-3}	4.22×10^{-2}	2.85×10^{-2}	-1.24×10^{-2}

K_1	K_2	K_3
1.15×10^{-11}	0.6×10^{-11}	1.53×10^{-11}

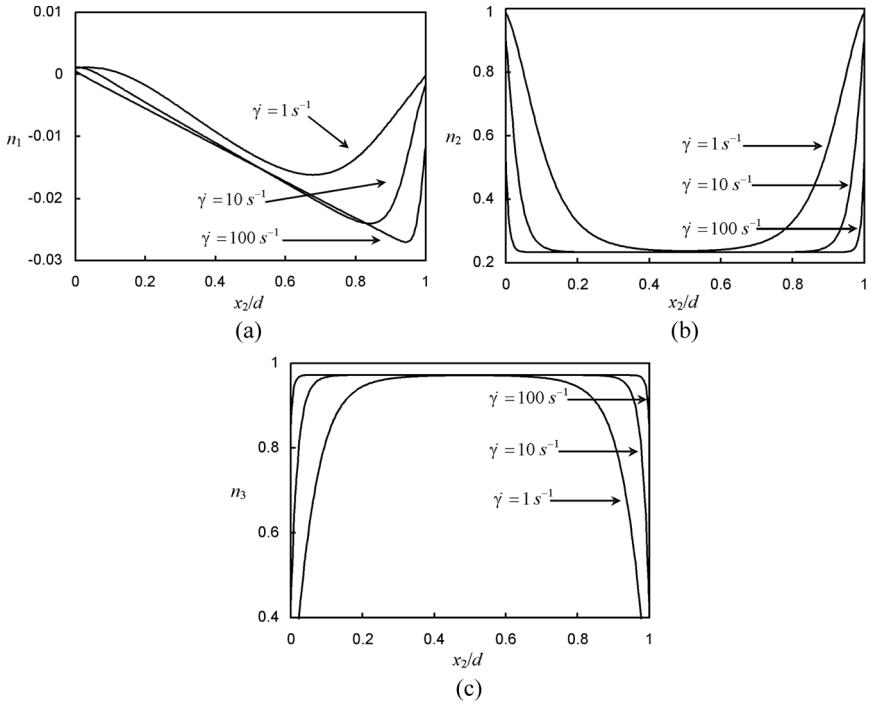

FIGURE 2 Steady director profile for MBBA at 40°C for two shear rates $\dot{\gamma}$. (a) component along the vorticity, (b) component along the symmetry axis of the cell, (c) component along the main velocity. The parameters used for the calculations are in Tables 1 and 2.

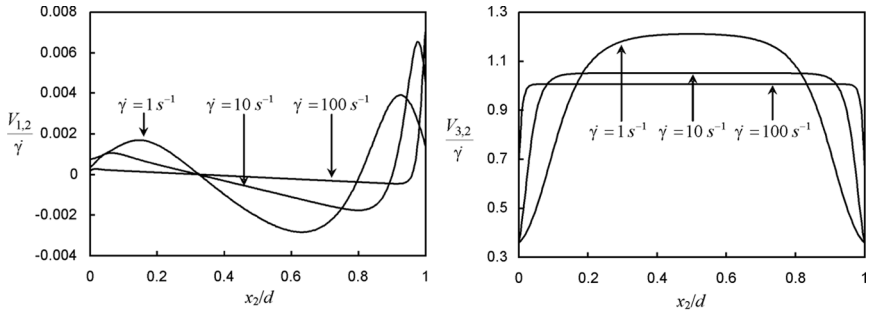

FIGURE 3 Steady profile of $V_{1,2}$ and $V_{3,2}$ for MBBA at 40°C in unit of $\dot{\gamma}$. The parameters used for the calculations are in Tables 1 and 2.

steady regime. As expected the velocity gradient $V_{3,2}$ is close to the nominal shear rate $\dot{\gamma}$ in the bulk (see Fig. 3b). It is however worth noting that $V_{3,2}$ is notably different from $\dot{\gamma}$ on the bounding plates (for instance we have $V_{3,2} \approx 0.4\,\dot{\gamma}$ for $\dot{\gamma} = 1\,\mathrm{s}^{-1}$ and $\dot{\gamma} = 10\,\mathrm{s}^{-1}$ in Fig. 3b). This feature led us to question the possibility of evaluating a quantity defined on the shearing surface from the flow characteristics of the bulk. On the other hand we note that $V_{1,2} << V_{3,2}$ and $V_{1,22} << V_{3,22}$, which indicates the weak weight of radial flow in front of the main flow. For that reason one might be tempted to fully neglect the radial flow in evaluating the normal force; actually this approach will appear to be wrong below.

Figure 5 shows the steady values of $\mathcal{N}_1$ and $\mathcal{N}_{1eff}$ evaluated on the cone in function of the shear rate $\dot{\gamma}$. The function $\mathcal{N}_1(\dot{\gamma})$ is simply a

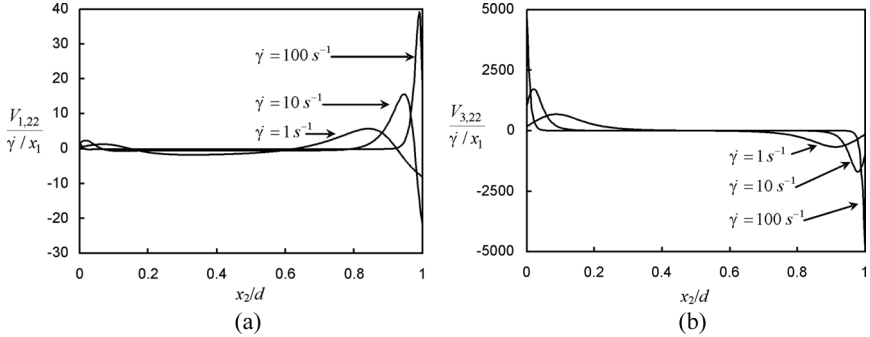

FIGURE 4 Steady profile of $V_{1,22}$ and $V_{3,22}$ for MBBA at 40°C in unit of $\dot{\gamma}/x_1$. The parameters used for the calculations are in Tables 1 and 2.

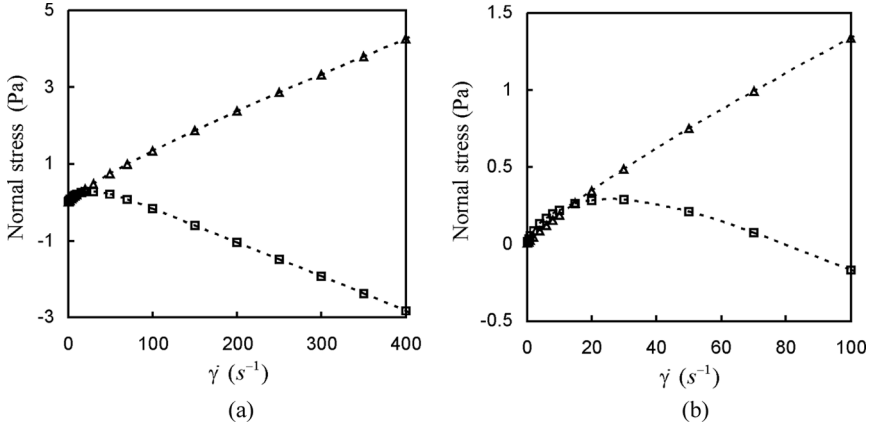

FIGURE 5 Steady normal stress difference *on the cone* in function of the shear rate $\dot{\gamma}$ for MBBA at 40°C: (□) effective normal stress difference $\mathcal{N}_{1eff}$ defined by Eq. (8), (△) pure normal stress difference $\mathcal{N}_1$ defined by Eq. (9). The parameters used for the calculations are in Tables 1 and 2.

quasi-linear positive and increasing function of $\dot{\gamma}$. On the contrary the function $\mathcal{N}_{1eff}(\dot{\gamma})$ is non-monotonous, it is positive and increasing until a threshold shear rate $\dot{\gamma}_1$ (that amounts to about $30\,s^{-1}$) while for $\dot{\gamma} \geq \dot{\gamma}_1$ the function starts to decrease until reaching a linear asymptotic regime characterized by negative slope and negative values. The main result is that $\mathcal{N}_{1eff}$ becomes notably different from $\mathcal{N}_1$ for $\dot{\gamma}$ above $\dot{\gamma}_1$, which emphasizes the importance of the component $\tau_{\theta r}$ (or τ_{21}) for liquid crystals. Figure 6 shows the same steady functions $\mathcal{N}_1$ and $\mathcal{N}_{1eff}$ but now evaluated in the middle of the gap instead of on the cone as in Figure 5. The comparison of Figures 5 and 6 shows that the values of $\mathcal{N}_1$ and $\mathcal{N}_{1eff}$ are significantly different between the middle gap and the bounding cone. This feature is also evidenced in Figure 7 that shows the strain dependence of $\mathcal{N}_{1eff}$ for a fixed shear rate on the cone and in the middle gap. It follows that one cannot use the simpler flow characteristics in the bulk to predict the normal force.

The Figures 8 and 9 show the shear viscosity response, i.e. the steady value of $\eta_{eff} = \sigma_{23}/\dot{\gamma}$ in function of $\dot{\gamma}$; in Figure 8 it is evaluated on the cone while in Figure 9 it is evaluated in the middle gap. Actually, unlike $\mathcal{N}_{1eff}$, no notable difference is observed for the shear viscosity between the middle gap and the cone. The main characteristic of the shear viscosity is a rapid decreasing for low shear rate followed by a constant value for higher shear rate. The interpretation of the shear viscosity response is straightforward. Initially the director

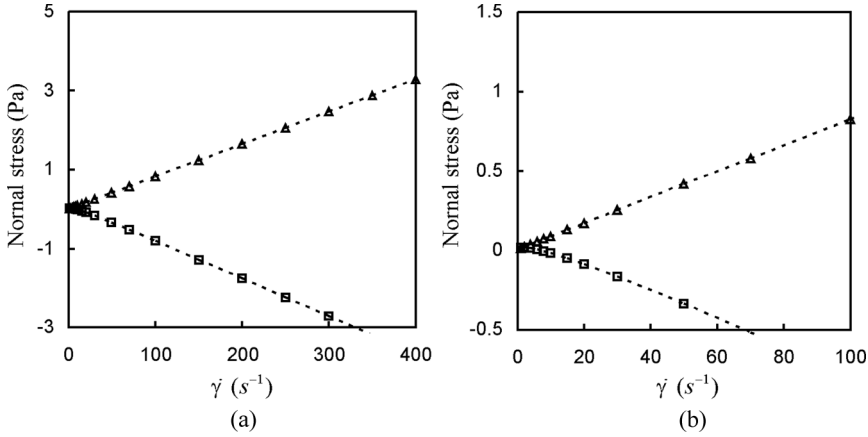

FIGURE 6 Steady normal stress difference *in the middle gap* in function of the shear rate $\dot{\gamma}$ for MBBA at 40°C: (□) effective normal stress difference $\mathcal{N}_{1eff}$ defined by Eq. (8), (△) pure normal stress difference $\mathcal{N}_1$ defined by Eq. (9). The parameters used for the calculations are in Tables 1 and 2. The axes are identical to those of Figure 5 in order to compare Figures 5 and 6, i.e. $\mathcal{N}_{1eff}$ and $\mathcal{N}_1$ in the bulk and on the cone.

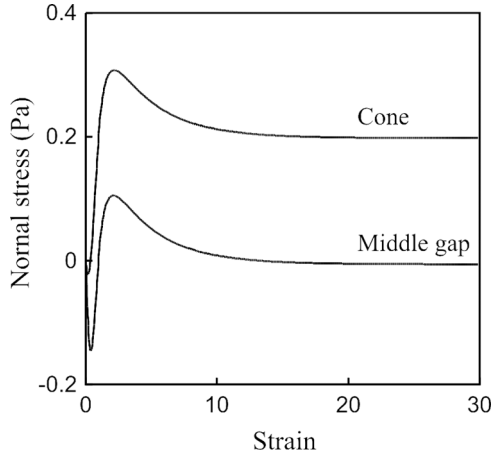

FIGURE 7 Strain dependence of the effective normal stress difference $\mathcal{N}_{1eff}$ defined by Eq. (8) on the cone (upper curve) and in the middle gap (lower curve) for MBBA at 40°C and for $\dot{\gamma} = 8\,s^{-1}$. The parameters used for the calculations are in Tables 1 and 2.

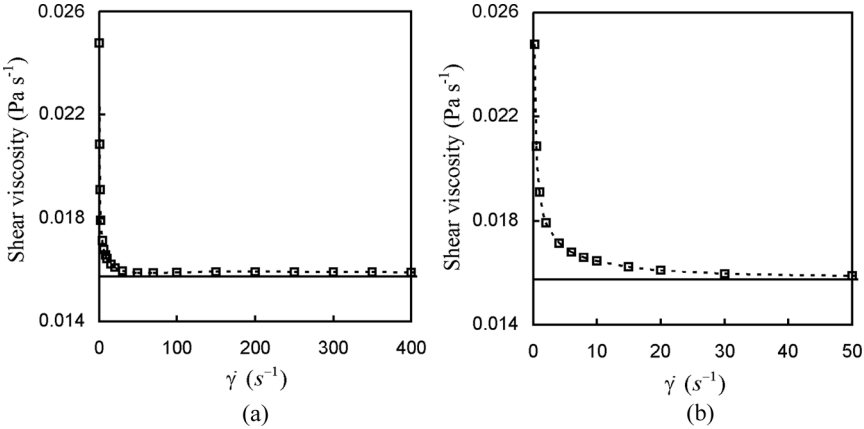

FIGURE 8 Steady shear viscosity $\eta_{eff} = \sigma_{23}/\dot{\gamma}$ *on the cone* in function of the shear rate $\dot{\gamma}$ for MBBA at 40°C: (□) shear viscosity predicted by the model, (—) analytical shear viscosity defined by Eq. (32). The parameters used for the calculations are in Tables 1 and 2.

is aligned with the easy axis defined in Table 1 ($n_1 \approx 0$, $n_2 \approx 1$, $n_3 \approx 0$) and consequently it is almost normal to the main velocity. The flow tends to align the director with a direction close to the main velocity

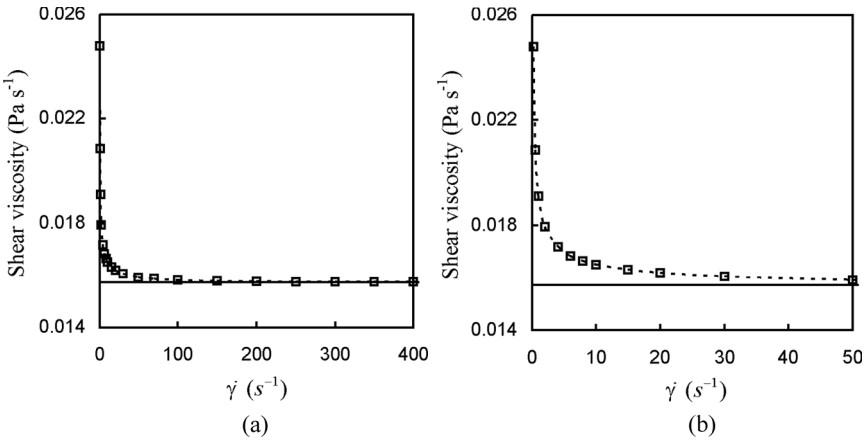

FIGURE 9 Steady shear viscosity $\eta_{eff} = \sigma_{23}/\dot{\gamma}$ *in the middle gap* in function of the shear rate $\dot{\gamma}$ for MBBA at 40°C: (□) shear viscosity predicted by the model, (—) analytical shear viscosity defined by Eq. (32). The parameters used for the calculations are in Tables 1 and 2.

direction (i.e. $n_1 \approx 0$ $n_2 \approx \sin\theta_L$ and $n_3 \approx \cos\theta_L$ where θ_L is the Leslie angle defined by $\tan\theta_L = \sqrt{\alpha_3/\alpha_2}$) but this feature is hindered by director anchoring. Accordingly, the shear must be sufficiently strong to effectively align the director close to the velocity in most part of the sample; actually the Figure 2c already illustrated this feature. Thus, at very low shear rate the steady director stays almost normal to the velocity and the effective shear viscosity is close to the Miesowicz viscosity $\eta_c = (\alpha_4 + \alpha_5 - \alpha_2)/2$ while for high shear rate the director aligns close to the velocity in most part of the sample and the effective shear viscosity is almost $\eta_b = (\alpha_4 + \alpha_6 - \alpha_3)/2$. Remarking that in practice η_c is notably higher than η_b the effective shear viscosity is expected to decrease from η_c to η_b when the shear rate increases and this decay reflects the increase of the alignment of the director with the velocity. It is worth comparing the shear viscosity predicted by the current model with the analytical shear viscosity obtained by simply applying the definition of the viscous stress assuming one single non-null velocity gradient, namely, $V_{3,2} = \dot{\gamma}$. Use of Eqs. (14) and (15) with $S_{ij} = 0$ yields

$$\eta_{eff} = L_{2332} = \frac{1}{2}(2\alpha_1 n_2^2 n_3^2 + \alpha_4 + (\alpha_5 - \alpha_2)n_2^2 + (\alpha_6 + \alpha_3)n_3^2) \tag{32}$$

with $n_2 = \sin\theta_L$ and $n_3 = \cos\theta_L$. This theoretical value is represented by a horizontal line in Figures 8 and 9. It appears that Eq. (32) yields an excellent estimation of the asymptotic shear viscosity, i.e. for shear rate above about $30\,\mathrm{s}^{-1}$.

A Cartesian expression for $\Delta\mathcal{N}_1$ is obtained by converting Eq. (10) to Cartesian coordinates with the help of Eqs. (II-1) and (II-2). Assuming moreover $\sin\theta \approx 1$, $\cos\theta \approx 0$ and $r \approx x_1$ we get

$$\Delta\mathcal{N}_1 \approx \tau_{11} - \tau_{22} - x_1 \frac{\partial \tau_{21}}{\partial x_2} \tag{33}$$

According to Eq. (24) the contribution $x_1 \partial\tau_{21}/\partial x_2$ to $\Delta\mathcal{N}_1$ may be decomposed into a sum of several terms whose values on the cone are reported in Table 3 for three shear rates in order to estimate their relative magnitude. The term $x_1 L^{\#}_{211} V_1$ vanishes exactly on the cone because of the boundary condition for V_1 (i.e. $V_1 = 0$). It appears that the two terms $x_1 L^{\#}_{213} V_3$ and $x_1 L^{\#}_{21122} V_{1,22}$ are dominant at any shear rate while for high shear rate $x_1 L^{\#}_{2112} V_{1,2}$ and $x_1 L^{\#}_{21322} V_{3,22}$ become dominant as well. The large magnitude of $x_1 L^{\#}_{213} V_3$ is easily understandable, it is because (i) V_3 is the main velocity component and (ii) strong director gradients are included in the coefficient $L^{\#}_{213}$ (see Eq. (26)). The most surprising result is the importance of the term $x_1 L^{\#}_{21122} V_{1,22}$ since (i) no director gradient

TABLE 3 Relative Magnitude of the Different Terms in $\mathcal{N}_{1eff}$ for Different Shear Rates According to Eqs. (8) and (24). The Terms are Evaluated on the Cone and η Denotes an Effective Viscosity Defined by $\eta = (\eta_b + \eta_c)/2$ where η_a and η_b are Miesowicz Viscosities

	$\dot{\gamma} = 1\,s^{-1}$	$\dot{\gamma} = 10\,s^{-1}$	$\dot{\gamma} = 100\,s^{-1}$
$x_1 L^{\#}_{211} V_1/\eta\dot{\gamma}$	0.00	0.00	0.00
$x_1 L^{\#}_{2112} V_{1,2}/\eta\dot{\gamma}$	0.68	12.89	30.81
$x_1 L^{\#}_{21122} V_{1,22}/\eta\dot{\gamma}$	−12.71	−30.77	16.19
$x_1 L^{\#}_{213} V_3/\eta\dot{\gamma}$	12.17	19.85	−19.18
$x_1 L^{\#}_{2132} V_{3,2}/\eta\dot{\gamma}$	−0.31	−1.80	−7.14
$x_1 L^{\#}_{21322} V_{3,22}/\eta\dot{\gamma}$	-2.19×10^{-3}	−0.25	−12.39
$(1/\eta\dot{\gamma})(x_1 \partial S_{21}/\partial x_2)$	6.62×10^{-10}	1.34×10^{-6}	-5.74×10^{-6}
$(1\eta\dot{\gamma})(x_1 \partial \tau_{21} \partial x_2)$	−0.17	-8.41×10^{-2}	8.30
$(\tau_{11} - \tau_{22})/\eta\dot{\gamma}$	0.67	0.44	0.18
$\mathcal{N}_1/\eta\dot{\gamma}$	0.72	0.55	0.39
$\tau_{21}/\eta\dot{\gamma}$	7.63×10^{-4}	3.19×10^{-3}	4.20×10^{-3}

arise in the coefficient $L^{\#}_{21122}$ (see Eq. (26)) and (ii) $V_{1,22} \ll V_{3,22}$ (see Fig. 4), Thus, despite $V_{1,22} << V_{3,22}$ the contribution associated to $V_{1,22}$ is larger or comparable to the one associated to $V_{3,22}$; it is partially because the coefficient $L^{\#}_{21322} = L_{2132}$ is much smaller than $L^{\#}_{21122} = L_{2112}$. Indeed, according to the definition, i.e. Eq. (15), we have $L_{2132} \approx 0$ and $L_{2112} \approx \alpha_{4/2}$ when $n_1 \approx 0$ and $n_2 \approx 0$.[6] Another important feature deserves to be pointed out: the sum of the dominant terms almost cancels, which entrains that *a-priori* non-dominant terms cannot be neglected without strongly affecting the final evaluation of $x_1 \partial \tau_{21}/\partial x_2$. For instance, the terms $x_1 L^{\#}_{2112} V_{1,2}$ and $x_1 L^{\#}_{2132} V_{3,2}$ for $\dot{\gamma} = 1\,\mathrm{s}^{-1}$ cannot be neglected although not dominant, likewise $x_1 L^{\#}_{2132} V_{3,2}$ for $\dot{\gamma} = 100\,\mathrm{s}^{-1}$. It turns out that the single term that can be neglected in $x_1 \partial S_{21}/\partial x_2$ is $x_1 \partial \delta_{21}/\partial x_2$. Thus the analysis of data in Table 3 reveals that the radial velocity although very small strongly contributes to the normal force through its first and second derivatives $V_{1,2}$ and $V_{1,22}$. That evidences, once again, that the normal force is extremely sensitive to the details of the flow within the boundary layers in contact with the cone. We have also reported in Table 3 the values of $\tau_{11} - \tau_{22}$ (that contribute to $\Delta\mathcal{N}_1$, see Eq. (33)), $\mathcal{N}_1$ and τ_{21}. It appears that $x_1 \partial \tau_{21}/\partial x_2$ is the dominant contribution to $\mathcal{N}_{1eff}$ for high shear rate and, moreover, this contribution is at the origin of the negative values of $\mathcal{N}_{1eff}$. On the other

[6]From Eq. (15) we have $L_{2132} = (2\alpha_1 n_2^2 + \alpha_6 + \alpha_3) n_1 n_3/2$ and $L_{2112} = \alpha_4/2 + (2\alpha_1 n_1^2 n_2^2 + (\alpha_5 - \alpha_2) n_2^2 + (\alpha_6 + \alpha_3) n_1^2)/2$.

hand we note that τ_{21} is actually much smaller than $\mathcal{N}_1$ or $(\tau_{11} - \tau_{22})$ while $x_1 \partial \tau_{21}/\partial x_2$ is dominant in $\mathcal{N}_{1eff}$. Accordingly, one must be careful in dropping a tensor component on the sole basis that it is negligible in front of the other ones.

V. CONCLUSION

The flow of nematics within a cone-and-plate cell has been investigated under four hypotheses: (i) incompressibility, (ii) negligible inertia, (iii) axial symmetry and (iv) radial invariance of the extra stress tensor. Our objective was to predict the normal force measured with a cone-and-plate set-up for nematic liquid crystals within the framework of Leslie-Ericksen theory. To this end we first derived a general expression for the normal force based on hypotheses (ii) to (iv). It has been found that the normal force is not simply proportional to the first normal stress difference $\mathcal{N}_1$ but instead to an 'effective first normal stress difference' $\mathcal{N}_{1eff} = \mathcal{N}_1 + \Delta\mathcal{N}_1$ where $\Delta\mathcal{N}_1$ is related to a spatial derivative of one stress tensor component in spherical coordinates. Subsequently we derived from the general Leslie-Ericksen theory an effective one-dimensional model describing the flow of nematics within a cone-and-plate cell in order to evaluate $\mathcal{N}_{1eff}$ for one particular material for which the Leslie viscosities are known, namely, MBBA.

The main results of this work are: (i) the additional contribution $\Delta\mathcal{N}_1$ is not negligible in front of $\mathcal{N}_1$, for MBBA, and (ii) $\Delta\mathcal{N}_1$ makes the normal force, Eq. (7), negative at high shear rate; more precisely it is the contribution $x_1 \partial \tau_{21}/\partial x_2$ to $\Delta\mathcal{N}_1$ that entrains $N_{1eff} < 0$. Two other significant results have been evidenced as well: (i) the importance of the radial flow in the magnitude of the normal force, despite a small radial velocity, and (ii) the fact that $\mathcal{N}_{1eff}$ on the cone surface differs notably from $\mathcal{N}_{1eff}$ in the bulk. Accordingly, it appears quite difficult to evaluate the normal force with a simple model, since some knowledge of the details of the flow in the vicinity of the bounding plates seems necessary. By comparison, the evaluation of the shear viscosity appears to be much easier since a very simple model yields a good estimate for sufficiently high shear rate (in the plateau region of the shear stress response). It is worth noting as well that it is not possible to evaluate $\Delta\mathcal{N}_1$ with the simple infinite parallel plates model because this model corresponds to the limit $x_1 \to \infty$ and $x_1 \partial \tau_{21}/\partial x_2 \to 0$ of the cone-and-plate model so that the product $x_1 \partial \tau_{21}/\partial x_2$, essential to evaluate $\Delta\mathcal{N}_1$, is indeterminate in this case.

APPENDIX I : GRADIENTS RESULTING FROM AXIAL SYMMETRY

In this Appendix we give expressions for the derivatives $\left.\frac{\partial T_{ij..}}{\partial x_3}\right|_{x_3=0}$ $(i, j, \ldots = 1, 2, 3)$ where T denotes a tensor field invariant under any rotation about the x_2 axis.

In order to evaluate these derivatives we use the fact that the components $T_{ij..}$ at two points M_1 and M_2 related by a rotation about the symmetry axis (i.e. the x_2 axis) are related as well according to the law of transformation defining tensors. On the other hand, to each point $M_1(x_1, x_2, \delta x_3)$ corresponds a point $M_2(x_1 + \delta x_1, x_2, 0)$ within the plane $(x_1 x_2)$ image of M_1 by a particular rotation about the x_2 axis; since actually two points M_2 satisfy this condition we consider the one that is close to M_1 when δx_3 is small so that δx_1 is a well-defined function of δx_3 that vanishes when δx_3 vanishes. Accordingly the variation $\Delta T_{ij..} = T_{ij\ldots}(x_1, x_2, \delta x_3) - T_{ij..}(x_1, x_2, 0)$ along x_3 may be expressed as $\Delta T_{ij\ldots} = R_{ik} R_{jl} \ldots T_{kl\ldots}(x_1 + \delta x_1, x_2, 0) - T_{ij\ldots}(x_1, x_2, 0)$ where $R_{\mathrm{pq}}(p,\ q = 1,\ 2,\ 3)$ denotes the components of the rotation matrix that transforms M_1 into M_2 and consequently they are well-defined functions of δx_3 as well. Finally the limits $\frac{\Delta T_{ij..}(x_1, x_2, \delta x_3)}{\delta x_3}$ $(i, j, \ldots = 1, 2, 3)$ when δx_3 approaches zero become calculable.

For the components $V_{\mathrm{i}} (i = 1,\ 2,\ 3)$ of a vector we have

$$\begin{cases} \frac{\partial V_1}{\partial x_3}\big|_{x_3=0} = -\frac{V_3}{x_1} \\ \frac{\partial V_2}{\partial x_3}\big|_{x_3=0} = 0 \\ \frac{\partial V_3}{\partial x_3}\big|_{x_3=0} = \frac{V_1}{x_1} \end{cases} \tag{I-1}$$

For the components $T_{ij}\,(i, j = 1, 2, 3)$ of a second rank tensor we have

$$\begin{cases} \frac{\partial T_{11}}{\partial x_3}\big|_{x_3=0} = -\frac{T_{13}+T_{31}}{x_1} \\ \frac{\partial T_{12}}{\partial x_3}\big|_{x_3=0} = -\frac{T_{32}}{x_1} \\ \frac{\partial T_{13}}{\partial x_3}\big|_{x_3=0} = \frac{T_{11}-T_{33}}{x_1} \end{cases} \quad \begin{cases} \frac{\partial T_{21}}{\partial x_3}\big|_{x_3=0} = -\frac{T_{23}}{x_1} \\ \frac{\partial T_{22}}{\partial x_3}\big|_{x_3=0} = 0 \\ \frac{\partial T_{23}}{\partial x_3}\big|_{x_3=0} = \frac{T_{21}}{x_1} \end{cases} \quad \begin{cases} \frac{\partial T_{31}}{\partial x_3}\big|_{x_3=0} = \frac{T_{11}-T_{33}}{x_1} \\ \frac{\partial T_{32}}{\partial x_3}\big|_{x_3=0} = \frac{T_{12}}{x_1} \\ \frac{\partial T_{33}}{\partial x_3}\big|_{x_3=0} = \frac{T_{13}+T_{31}}{x_1} \end{cases} \tag{I-2}$$

When Eqs. (I-1) and (I-2) are applied to the particular second rank tensor $T_{ij} = V_{ij}\ (i,\ j = 1, 2, 3)$ we get

$$\begin{cases} \frac{\partial V_{1,1}}{\partial x_3}\big|_{x_3=0} = \frac{V_3}{x_1^2} - \frac{V_{3,1}}{x_1} \\ \frac{\partial V_{1,2}}{\partial x_3}\big|_{x_3=0} = -\frac{V_{3,2}}{x_1} \\ \frac{\partial V_{1,3}}{\partial x_3}\big|_{x_3=0} = -\frac{V_1}{x_1^2} + \frac{V_{1,1}}{x_1} \end{cases} \quad \begin{cases} \frac{\partial V_{2,1}}{\partial x_3}\big|_{x_3=0} = 0 \\ \frac{\partial V_{2,2}}{\partial x_3}\big|_{x_3=0} = 0 \\ \frac{\partial V_{2,3}}{\partial x_3}\big|_{x_3=0} = \frac{V_{2,1}}{x_1} \end{cases} \quad \begin{cases} \frac{\partial V_{3,1}}{\partial x_3}\big|_{x_3=0} = -\frac{V_1}{x_1^2} + \frac{V_{1,1}}{x_1} \\ \frac{\partial V_{3,2}}{\partial x_3}\big|_{x_3=0} = \frac{V_{1,2}}{x_1} \\ \frac{\partial V_{3,3}}{\partial x_3}\big|_{x_3=0} = -\frac{V_3}{x_1^2} + \frac{V_{3,1}}{x_1} \end{cases} \tag{I-3}$$

APPENDIX II: RELATION BETWEEN SPHERICAL AND CARTESIAN COMPONENTS OF TENSORS

We give here the expressions of some spherical components $T_{\alpha\beta}$ (α, $\beta = r,\ \theta,\ \phi$) of a tensor in function of Cartesian components T_{ij} ($i,\ j = 1, 2, 3$). The relations are valid when the tensor T is evaluated at a point belonging to the plane $x_3 = 0$. In this case the local basis vectors associated with spherical coordinates are $\vec{e}_r = \sin\theta\vec{e}_1 + \cos\theta\vec{e}_2$, $\vec{e}_\theta = \cos\theta\vec{e}_1 - \sin\theta\vec{e}_2$ and $\vec{e}_\phi = -\vec{e}_3$. We have

$$\begin{cases} T_{rr} = \sin^2\theta T_{11} + \sin\theta\cos\theta(T_{12} + T_{21}) + \cos^2\theta T_{22} \\ T_{\theta\theta} = \cos^2\theta T_{11} - \sin\theta\cos\theta(T_{12} + T_{21}) + \sin^2\theta T_{22} \\ T_{\phi\phi} = T_{33} \\ T_{\theta r} = \sin\theta\cos\theta(T_{11} - T_{22}) + \cos^2\theta T_{12} - \sin^2\theta T_{21} \\ T_{r\phi} = -\sin\theta T_{13} - \cos\theta T_{23} \\ T_{\phi r} = -\sin\theta T_{31} - \cos\theta T_{32} \\ T_{\theta\phi} = -\cos\theta T_{13} + \sin\theta T_{23} \end{cases} \tag{II-1}$$

Hence we readily get

$$\begin{aligned} \frac{\partial T_{\theta r}}{\partial\theta} &= \cos^2\theta(T_{11} - T_{22}) - \sin^2\theta(T_{11} - T_{22}) - 2\sin\theta\cos\theta(T_{12} + T_{21}) \\ &\quad + r\sin\theta\cos\theta\left(\cos\theta\frac{\partial T_{11}}{\partial x_1} - \sin\theta\frac{\partial T_{11}}{\partial x_2} - \cos\theta\frac{\partial T_{22}}{\partial x_1} + \sin\theta\frac{\partial T_{22}}{\partial x_2}\right) \\ &\quad + r\cos^2\theta\left(\cos\theta\frac{\partial T_{12}}{\partial x_1} - \sin\theta\frac{\partial T_{12}}{\partial x_2}\right) \\ &\quad - r\sin^2\theta\left(\cos\theta\frac{\partial T_{21}}{\partial x_1} - \sin\theta\frac{\partial T_{21}}{\partial x_2}\right) \end{aligned} \tag{II-2}$$

and

$$\begin{aligned} \frac{\partial T_{\theta\phi}}{\partial\theta} &= \sin\theta T_{13} + \cos\theta T_{23} - r\cos\theta\left(\cos\theta\frac{\partial T_{13}}{\partial x_1} - \sin\theta\frac{\partial T_{13}}{\partial x_2}\right) \\ &\quad + r\sin\theta\left(\cos\theta\frac{\partial T_{23}}{\partial x_1} - \sin\theta\frac{\partial T_{23}}{\partial x_2}\right) \end{aligned} \tag{II-3}$$

APPENDIX III: VELOCITY GRADIENTS

The aim of this Appendix is to express all the first and second spatial derivatives of the components V_1 and V_3 of the velocity (other than $V_{1,2}$, $V_{1,22}$, $V_{3,2}$, $V_{3,22}$) when axial symmetry, incompressibility condition, $V_2 = 0$ and Eq. (22) are taken into account.

When $V_2 = 0$ the incompressibility condition yields

$$V_{1,1} = -V_{3,3} \tag{III-1}$$

By differentiating Eq. (III-1) with respect to x_1 and x_2 we get

$$\begin{cases} V_{1,11} = -V_{3,31} \\ V_{1,12} = -V_{3,32} \end{cases} \tag{III-2}$$

By combining Eqs. (III-1), (III-2) with Eqs. (I-1) and (I-3) resulting from axial symmetry and the assumption of the model expressed by Eq. (22) we get

$$\begin{cases} V_{1,1} = -V_1/x_1 \\ V_{1,3} = -V_3/x_1 \\ V_{3,3} = V_1/x_1 \end{cases} \tag{III-3}$$

$$\begin{cases} V_{1,11} = 2V_1/x_1^2 \\ V_{1,12} = -V_{1,2}/x_1 \\ V_{1,13} = 0 \end{cases} \qquad \begin{cases} V_{1,31} = 0 \\ V_{1,32} = -V_{3,2}/x_1 \\ V_{1,33} = -2V_1/x_1^2 \end{cases} \tag{III-4}$$

$$\begin{cases} V_{3,11} = 0 \\ V_{3,12} = 0 \\ V_{3,13} = -2V_1/x_1^2 \end{cases} \qquad \begin{cases} V_{3,31} = -2V_1/x_1^2 \\ V_{3,32} = V_{1,2}/x_1 \\ V_{3,33} = 0 \end{cases} \tag{III-5}$$

APPENDIX IV: BOUNDARY CONDITIONS FOR THE DIRECTOR

When, in addition to the volume free energy density associated with Frank elasticity, a surface energy density of Rapini-Papoular type [9] with strength A_s and easy axis $\vec{e}$ is assumed the minimization of the total energy leads to

$$(K_2 u_j + (K_3 - K_2)(\vec{n}\cdot\vec{u})n_j)n_{i,j} + (K_1 - K_2)(u_i - (\vec{n}\cdot\vec{u})n_i)n_{j,j} = h_{si}^{\perp} \quad i = 1,2,3 \tag{IV-1}$$

on the boundaries[7]. In Eq. (IV-1) $\vec{u}$ denotes the outward unit vector normal to the boundary and $\vec{h}_s^{\perp}$ is defined by

$$\vec{h}_s^{\perp} = A_s(\vec{e}\cdot\vec{n})\vec{e}^{\perp} \tag{IV-2}$$

with

$$\vec{e}^{\perp} = \vec{e} - (\vec{e}\cdot\vec{n})\vec{n} \tag{IV-3}$$

[7]The mathematical foundations leading to Eq. (IV-1) may be found in [10].

For plates normal to the x_2 axis we have $u_1 = 0$, $u_2 = \pm 1$ and $u_3 = 0$; accordingly Eq. (IV-1) yields

$$\begin{cases} K_{31}n_1n_2n_{1,1} + [K_2 + K_{32}n_2^2]n_{1,2} - K_{12}n_1n_2n_{2,2} \\ \quad + K_{32}n_2n_3n_{1,3} - K_{12}n_1n_2n_{3,3} = u_2h_{s1}^{\perp} \\ K_{12}(1 - n_2^2)n_{1,1} + K_{32}n_1n_2n_{2,1} + [K_1 + K_{31}n_2^2]n_{2,2} + K_{32}n_2n_3n_{2,3} \\ \quad + K_{12}(1 - n_2^2)n_{3,3} = u_2h_{s2}^{\perp} \\ -K_{12}n_2n_3n_{1,1} + K_{32}n_1n_2n_{3,1} - K_{12}n_2n_3n_{2,2} \\ \quad + [K_2 + K_{32}n_2^2]n_{3,2} + K_{31}n_2n_3n_{3,3} = u_2h_{s3}^{\perp} \end{cases} \tag{IV-4}$$

where the following notations $K_{12} = K_1 - K_2$, $K_{32} = K_3 - K_2$ and $K_{31} = K_3 - K_1$ have been used. With $\partial\vec{n}/\partial x_1 = \vec{0}$ assumed in section III-2 and $\partial\vec{n}/\partial x_3$ given by Eq. (I-1) we get

$$\begin{cases} [K_1 + K_{31}n_2^2]n_{2,2} = u_2h_{s2}^{\perp} - K_{12}(1 - n_2^2)n_1/x_1 \\ [K_2 + K_{32}n_2^2]n_{3,2} = u_2h_{s3}^{\perp} - K_{31}n_1n_2n_3/x_1 + K_{12}n_2n_3n_{2,2} \\ [K_2 + K_{32}n_2^2]n_{1,2} = u_2h_{s1}^{\perp} + K_{32}n_2n_3^2/x_1 + K_{12}n_1^2n_2/x_1 + K_{12}n_1n_2n_{2,2} \end{cases} \tag{IV-5}$$

These equations constitute the boundary conditions for the director.

REFERENCES

[1] Malvern, L. E. (1969). *Introduction to the Mechanics of a Continuous Medium*. Prentice-Hall: New Jersey.

[2] Leslie, F. M. (1968). *Arch. Rat. Mech. Anal.*, *28*, 265.

[3] De Gennes, P. G. & Prost, J. (1993). *The Physics of Liquid Crystals*. 2nd ed., Oxford University Press: Oxford.

[4] Véron, A. & Martins, A. F. (2005). *Mol. Cryst. Liq. Cryst.*, *435*, 199.

[5] Fletcher, C. A. J. (1991). *Computational Techniques for Fluid Dynamics*. 2nd ed., Springer Series in Computational Physics, Springer-Verlag: Heidelberg.

[6] Blinov, L. M., Kabayenkov, A. Yu., & Sonin, A. A. (1989). *Liq. Cryst.*, *5*, 645.

[7] Kneppe, H., Schneider, F., & Sharma, N. K. (1981). *Ber. Bunsenges. Phys. Chem.*, *85*, 784; Kneppe, H., Schneider, F., & Sharma, N. K. (1982). *J. Chem. Phys.*, *77*, 3203.

[8] Karat, P. P. & Madhusudana, N. V. (1977). *Mol. Cryst. Liq. Cryst.*, *40*, 239.

[9] Rapini, A. & Papoular, M. (1969). *J. Phys. (Paris)*, *30C*, 4.

[10] Mikhlin, S. G. (1970). *Mathematical Physics, an Advanced Course*. North-Holland series in Applied Mathematics and Mechanics, North-Holland publishing co.: Amsterdam.